# Development of a mathematical model for the study of transients in general primary frequency control in power systems

*Viktoriya* Fyodorova[1], *Viktor* Kirichenko[1], and *Gleb* Glazyrin[1]

[1]Novosibirsk State Technical University, 630073, Novosibirsk, Russian Federation

**Abstract.** General primary frequency regulation (GPFR) is employed within the power system to limit frequency variation deviations from a reference value in positive and negative directions, ensuring safe power object operations and reducing the prevalence of power outages. Specific requirements outlined in normative documents must be met when carrying out GPFR procedures. However, in practice, frequency regulation is beset by a range of issues. Certain emergency disturbances induce undamped frequency fluctuations and unwarranted customer and generator outages. A striking illustration of this phenomenon is provided by the Norilsk-Taimyr power system mishap involving an imbalanced active power of 40 MW. Low-frequency oscillations persisted for nearly 30 seconds, and stable GPFR operation was only achieved at a rate equivalent to 25 %, which falls short of the stipulated standards. This study highlights the issue of suboptimal GPFR laws for controlling frequency in a power system with multiple frequency-leading power plants. The Norilsk-Taimyr power system is modelled using MATLAB to investigate transients in GPFR. The results identify shortcomings in the current control laws and provide criteria for developing updated control algorithms.

## 1 Introduction

General Primary Frequency Regulation (GPFR) refers to the automated adjustment of the power output from generating equipment, carried out by dedicated controllers in response to fluctuations in frequency in order to reduce said fluctuations. Primary controllers, including automatic speed controllers and active power controllers, are utilised to perform primary regulation of the generating equipment. Primary regulation should prioritise limiting deviation of frequency from the prescribed limit for use by the power plant, while also minimising the possibility of attracting power-consuming units. All generating equipment must comply with the participation requirements to take part in the power frequency control [1], [2].

The generator's frequency regulation occurs at different stages of its operation. Frequency regulation takes place during generator start-up and its connection to the grid for parallel operation, i.e., synchronisation. During operation, the generator frequency is regulated to prevent emergency situations in the power system. Additional information about the process of frequency regulation during synchronisation is available in references [3] and [4]. This

study examines the intricacies of regulating the mode characteristics of an operational generator to alter the frequency of the interlinked power system.

The effectiveness of primary frequency regulation by automatic control systems (ACS) of turbines is crucial to the quality of frequency, voltage, and current in the power system.

During real-life power system emergencies, undamped frequency oscillations (UFO) can occur in frequency control. This results in avoidable power outages for consumers and generation. Unfortunately, the operation of turbine control systems at some of the world's largest power plants has led to several accidents due to non-damped oscillations.

Extensive research has been conducted on the primary frequency control process, as reported in [5-7]. The authors investigated emergency situations with significant oscillations during frequency control in recent years. They noted that undamped oscillations were caused by frequency regulators with feedback on generator active power. Loss of power system stability can result from incorrect tuning of such regulators' parameters.

The problem of undamped frequency oscillations in power systems can be resolved by tuning turbine frequency regulators accordingly. Presently, most regulators utilise frequency correction according to the PI law, thus accurately modifying primary power when frequency value changes occur. However, optimal regulation stability is still potentially compromised, particularly in power systems that include several power plants involved in regulation.

An important issue is the analysis of the quality of the HDR process in systems with high hydroelectric power plants, because in most cases frequency regulation is carried out by these types of generating equipment due to their manoeuvrability. The works [8-12] consider this problem. The authors studied frequency fluctuations in several power systems with a high share of hydro generation. The papers describe the regime in a power system with several hydroelectric power plants, which led to a long period of ultra-low frequency oscillations, seriously affecting the safe and stable operation of the entire system. The authors evaluated the features of frequency regulation and found that the half-period characteristic of turbine counter-regulation leads to the occurrence of ultra-low frequency oscillations. Optimization and increase of efficiency of this process implies joint tuning of all controllers as a part of regulation systems.

Another measure to improve the efficiency of the FRA process is the installation of multifunction, multi-band stabilizers (MBS) [13-14]. Such MSSs allow to improve the control by means of a wide range of adjustable parameters and to obtain the required phase characteristics.

The analysis of existing research on GPFRs shows that the main measure to improve the primary frequency control performance is either fine tuning of the regulators or using better regulator models. However, it is important to consider this problem from the perspective of improving the control laws themselves. This paper is the first step in this direction and represents the creation of a multifunctional mathematical model as a prototype of the Norilsk-Taimyr power system.

The objectives of the research may be:

1. Analyse existing frequency control methods and devices for implementing GPFR;
2. Model the Norilsk-Taimyr power system, with the ability to set various control algorithms in automatic devices and study transients at GPFR through graphs;
3. Investigate the stability and quality of GPFR transients with varying laws of generating equipment control.

The paper is structured as follows: Section II outlines primary frequency control requirements for power systems, presents a mathematical model for the study of transients in the GPFR of power systems. The results of the simulation are discussed in Section III, and Section IV concludes the paper.

# 2 Methods

## 2.1 Requirements for primary frequency control of power systems

The primary regulation [15] imposes the following requirements:

• for generating equipment with turbines equipped with electro-hydraulic governors, the dead zone must not exceed 0.05 Hz, while for generating equipment with turbines equipped with hydraulic governors, it must not exceed 0.15 Hz;

• the dead zone for the primary regulation should not exceed (50±0.075) Hz;

• the primary control droop must be within 4–5 % of power units with steam and gas turbines, and within 4.5–6 % for hydraulic turbines.

Verification and confirmation of the generating equipment's preparedness for participating in the GPFR should follow the requirements of the power system's operator.

TPPs' generating equipment (excluding gas and steam turbines) must meet the following maneuvering characteristics.

If the frequency deviation is 10 % or less than the rated power of the generating equipment, it is necessary to guarantee the generating equipment's participation in the GPFR within the control range. In the event of a sudden frequency deviation, make sure to:

- provide at least half of the required primary power for a duration not exceeding 15 seconds;

- deliver all the required primary power within 5–7 minutes, depending on the type of power unit.

To participate in the GPFR, the HPP generating equipment's maneuvering characteristics must meet specific requirements.

To guarantee participation, the generating equipment must be able to operate within the entire control range during frequency deviation. Additionally, in case of a jump frequency deviation, the equipment should be able to implement the necessary primary power within one minute [16].

## 2.2 Description of the mathematical model for the study of GPFR transients

### *2.2.1 Mathematical model of a single-machine system*

Model development commences with the creation of a model of the hydro-generator using the mechanical and electrical specifications provided. As previously mentioned, the model will resemble the Norilsk-Taimyr power system and hence the modeling process will begin with Ust-Khantayskai HPP's hydro unit.

The authors of the article develop their own model of power system, since the existing mathematical models may lack both the generator frequency regulators and the possibility of their adjustment and variation of parameters, which is necessary for the problems of GPFR research. This choice was made due to possible limitations of current mathematical models, which may lack the necessary features for researching HPFD, such as generator frequency regulators. Technical abbreviations are defined upon first use.

The mechanical component is described and comprises the functions of the hydraulic turbine and actuator. To model the hydraulic turbine, a simplified transfer function (1) was utilized, which considered rigid hydraulic shock, clutch power, and the guide apparatus opening.

$$W_{em}(p) = \frac{1 - u_0 T_w p}{1 + 0.5 \cdot u_0 T_w p}, \quad (1)$$

where $u_0$ – initial opening of the guiding apparatus in per units; $T_w$ – conduit time constant.

The transfer function can be transformed into a differential equation (2) and written as:

$$\frac{dP_t}{dt} = \frac{2}{T_w} - 2\frac{dS_{wg}}{dt} - \frac{2}{T_w}\frac{P_t}{S_{wg}}. \quad (2)$$

In this equation, $S_{wg}$ represents the opening of the guiding apparatus.

An aperiodic link (3) was used as an approximate model of executing mechanisms, which is confirmed by experimental data (oscillograms of the Ust-Khantai HPP):

$$W_{em}(p) = \frac{1}{1+T_{em}p}. \quad (3)$$

Then the differential equation (4) describing the opening of the guide vane will be:

$$\frac{dS_{wg}}{dt} = \frac{x - S_{wg}}{T_{sm}} \quad (4)$$

where x – initial opening of guiding apparatus in per units; $T_{sm}$ – servomotor time constant.

The following equation is the rotor motion equation (5), which describes the external forces acting on the hydraulic unit rotor:

$$J\frac{d\omega}{dt} = M_{ext} + M_{syn} + M_{asyn}, \quad (5)$$

where J – inertia moment of rotating parts, ω – shaft angular frequency, $M_{in}$ – external mechanical torque on the synchronous machine shaft, $M_{syn}$ – synchronous electromagnetic torque, $M_{asyn}$ – asynchronous electromagnetic torque.

This stage of modelling is simplified where the asynchronous torque is deemed zero, the turbine torque is expressed in relation to the unit's rated power, and the synchronous torque is taken as equal to the load power, in the first approximation. The load power is expressed as the sum of the constant component and the frequency-dependent component considering the regulatory effect of the load. Friction losses are considered to be 2 % of the machine's rated power. The rotor motion equation (5) becomes (6) accordingly.

$$\frac{d\omega}{dt} = \frac{P}{\omega \cdot J} - \frac{P_{load}}{J} - K_{ml} \cdot \omega. \quad (6)$$

### *2.2.2 Mathematical model of a two-machine system*

At this stage of modeling, the electrical and mechanical parameters of the second unit are assumed to be equal to the parameters of the first.

To derive equations describing the processes in the stator circuit, an equivalent circuit has been drawn up (Fig. 1). Two synchronous machines connected to buses connected to an infinite power system through resistance $r_s+jx_s$. The busbars are also connected to a load with a constant resistance rl+jxl. As positive direction of machine currents ($I_d$, $I_q$) and system ($I_s$) the direction to the busbar is taken, for the load current ($I_l$) – from the busbar.

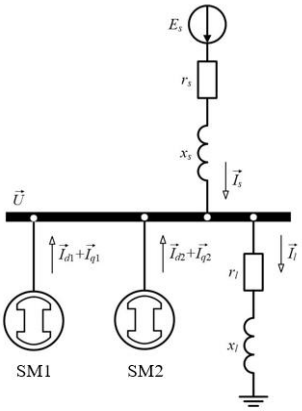


**Fig. 1.** Electrical equivalent circuit of two synchronous machines connected to busbars.

It is necessary to write equations according to the 1st and 2nd Kirchhoff laws for the circuit (Fig. 1) and the system of equations (7) relating currents, voltage and EMF of synchronous machines:

$$\begin{cases} \vec{I}_l = \vec{I}_{d1} + \vec{I}_{q1} + \vec{I}_{d2} + \vec{I}_{q2} + \vec{I}_s, \\ \vec{U} = \vec{E}_s - \vec{I}_s Z_s, \\ \vec{U} = \vec{I}_l Z_l, \\ \vec{U} = \vec{E}_1 - \vec{I}_{d1}\left(r_{a1} + jx_{d1}\right) - \vec{I}_{q1}\left(r_{a1} + jx_{q1}\right), \\ \vec{U} = \vec{E}_2 - \vec{I}_{d2}\left(r_{a2} + jx_{d2}\right) - \vec{I}_{q2}\left(r_{a2} + jx_{q2}\right). \end{cases} \quad (7)$$

where $E_s$ – phase EMF of the system, $Z_s$ – complex connection resistance with the system, $Z_l$ – complex load resistance, $E_1$ – phase EMF of the first synchronous machine, $E_2$ – phase EMF of the second synchronous machine, $r_{a1}$ – active resistance of the stator winding of the first machine, $r_{a2}$ – active resistance of the stator winding of the second machine, $x_{d1}$, $x_{q1}$ – inductive resistances of the stator winding along the longitudinal and transverse axes of the first machine, $x_{d2}$, $x_{q2}$ – inductive resistances of the stator winding along the longitudinal and transverse axes of the second machine.

Next, mathematical calculations will be presented to obtain an equation relating the electrical parameters of the first and second synchronous generators. The transition to the coordinate system in the d/q axes is shown in Figure 2.

From the first, second and third equations (7) we obtain equation (8):

$$\vec{I}_s = \frac{\vec{E}_s - \left(\vec{I}_{d1} + \vec{I}_{q1} + \vec{I}_{d2} + \vec{I}_{q2}\right) Z_l}{Z_l + Z_s} = \frac{\vec{E}_s}{Z_l + Z_s} - \left(\vec{I}_{d1} + \vec{I}_{q1} + \vec{I}_{d2} + \vec{I}_{q2}\right) \frac{Z_l}{Z_l + Z_s}. \quad (8)$$

From the second and fourth equations (7) we obtain equation (9):

$$\begin{aligned}\vec{I}_{d1}\left(r_{a1}+jx_{d1}+Z_{ls}\right)+\vec{I}_{q1}\left(r_{a1}+jx_{q1}+Z_{ls}\right)+\\+\vec{I}_{d2}Z_{ls}+\vec{I}_{q2}Z_{ls}=\vec{E}_1-\vec{E}_sK_{ls}.\end{aligned} \tag{9}$$

Similarly, from the second and fifth equations (7) we obtain equation (10):

$$\begin{aligned}\vec{I}_{d2}\left(r_{a2}+jx_{d2}+Z_{ls}\right)+\vec{I}_{q2}\left(r_{a2}+jx_{q2}+Z_{ls}\right)+\\+\vec{I}_{d1}Z_{ls}+\vec{I}_{q1}Z_{ls}=\vec{E}_2-\vec{E}_sK_{ls}.\end{aligned} \tag{10}$$

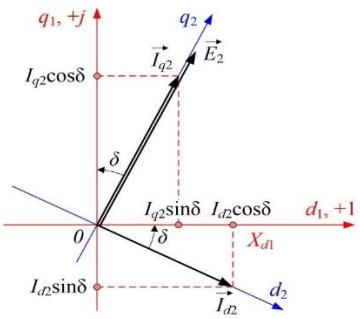


**Fig. 2.** Transition to coordinate system d/q (d1 – real axis, q1 – imaginary axis).

$$\begin{cases}\vec{I}_{d1}=I_{d1},\\ \vec{I}_{q1}=jI_{q1},\\ \vec{E}_1=jE_1,\\ \vec{I}_{d2}=I_{d2}\cos\delta-jI_{d2}\sin\delta=I_{d2}\left(\cos\delta-j\sin\delta\right),\\ \vec{I}_{q2}=I_{q2}\sin\delta+jI_{q2}\cos\delta=I_{q2}\left(\sin\delta+j\cos\delta\right),\\ \vec{E}_2=E_2\sin\delta+jE_2\cos\delta=E_2\left(\sin\delta+j\cos\delta\right),\\ \vec{E}_s=U_{\text{nom}}e^{j(90°-\delta_{1s})};\end{cases} \tag{11}$$

where $\delta_{1s}$ – angle between the EMF of the first synchronous machine and the EMF of the system ($\delta_{1s}=\alpha_1-\alpha_s$).

Introduce the following notation (12):

$$\begin{gathered}\vec{E}_x=\vec{E}_sK_{ls},E_{xr}=\text{Re}\left(\vec{E}_x\right),E_{xi}=\text{Im}\left(\vec{E}_x\right),\\ r_{ls}=\text{Re}\left(Z_{ls}\right),x_{ls}=\text{Im}\left(Z_{ls}\right),\\ r_{a1ls}=r_{a1}+r_{ls},x_{d1ls}=x_{d1}+x_{ls},x_{q1ls}=x_{q1}+x_{ls},\\ z_{ls\delta11}=r_{ls}\cos\delta+x_{ls}\sin\delta,z_{ls\delta12}=r_{ls}\sin\delta-x_{ls}\cos\delta,\\ r_{a2ls}=r_{a2}+r_{ls},x_{d2ls}=x_{d2}+x_{ls},x_{q2ls}=x_{q2}+x_{ls},\\ z_{ls\delta21}=r_{a2ls}\cos\delta+x_{d2ls}\sin\delta,z_{ls\delta22}=r_{a2ls}\sin\delta-x_{q2ls}\cos\delta,\\ z_{ls\delta23}=r_{a2ls}\sin\delta-x_{d2ls}\cos\delta,z_{ls\delta24}=r_{a2ls}\cos\delta+x_{q2ls}\sin\delta.\end{gathered} \tag{12}$$

Then, after a series of transformations of the system of equations (11), taking into account (12), we obtain a system of equations (13) for determining the currents of the first and second synchronous machines:

$$\begin{cases} I_{d1}r_{a1ls} - I_{q1}x_{q1ls} + I_{d2}z_{ls\delta 11} + I_{q2}z_{ls\delta 12} = -E_{xr}, \\ I_{d1}x_{d1ls} + I_{q1}r_{a1ls} - I_{d2}z_{ls\delta 12} + I_{q2}z_{ls\delta 11} = E_1 - E_{xi}, \\ I_{d1}r_{ls} - I_{q1}x_{ls} + I_{d2}z_{ls\delta 21} + I_{q2}z_{ls\delta 22} = E_2 \sin\delta - E_{xr}, \\ I_{d1}x_{ls} + I_{q1}r_{ls} - I_{d2}z_{ls\delta 23} + I_{q2}z_{ls\delta 24} = E_2 \cos\delta - E_{xi}. \end{cases} \quad (13)$$

The system of equations (13) in matrix form will look like (14):

$$\begin{bmatrix} r_{a1ls} & -x_{q1ls} & z_{ls\delta 11} & z_{ls\delta 12} \\ x_{d1ls} & r_{a1ls} & -z_{ls\delta 12} & z_{ls\delta 11} \\ r_{ls} & -x_{ls} & z_{ls\delta 21} & z_{ls\delta 22} \\ x_{ls} & r_{ls} & -z_{ls\delta 23} & z_{ls\delta 24} \end{bmatrix} \cdot \begin{bmatrix} I_{d1} \\ I_{q1} \\ I_{d2} \\ I_{q2} \end{bmatrix} = \begin{bmatrix} -E_{xr} \\ E_1 - E_{xi} \\ E_2 \sin\delta - E_{xr} \\ E_2 \cos\delta - E_{xi} \end{bmatrix} \quad (14)$$

To find the EMF of synchronous machines and solve the matrix equation 14, it is additionally necessary to introduce equations for the excitation circuits of both synchronous machines into the model. To describe the processes in the excitation circuit, the differential equation for the equilibrium of EMF and voltage drops (15) is used:

$$u_f = r_f i_f + L_{f\mu}\frac{di_f}{dt} + M_{fd\mu}\frac{dI_d}{dt}, \quad (15)$$

where $u_f$ – voltage on the excitation winding, $r_f$ – active resistance of the excitation winding, $i_f$ – excitation current, $L_{fd\mu}$ – own inductance of the excitation winding, taking into account saturation, $M_{fd\mu}$– mutual inductance, taking into account the saturation of the field winding and the stator winding (longitudinal circuit).

## 3 Results

The system of differential equations described by equations 2, 4, and 6 was solved using the ODE 45 solver within the MATLAB environment. The solution was obtained for the time interval from 0 to 60 seconds with a step size of 0.01 seconds and is displayed in Figure 3. The model functions correctly, as demonstrated by the figure. Increasing the opening of the guide vane (expressed as a percentage) results in a corresponding increase in the active power output of the unit (measured in p.u.).

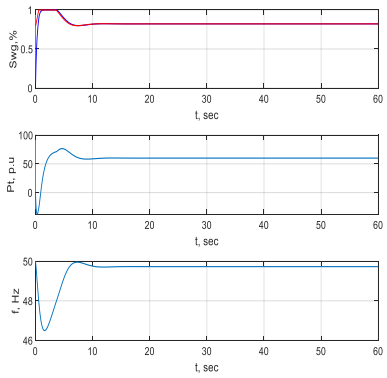


**Fig. 3.** The result of the functioning of a mathematical model containing one synchronous machine.

Additionally, to evaluate transient processes in implementing the GPFR, it is crucial to develop a mathematical model for a two-machine power system.

This involves expanding the current model by:

1. Incorporating equations for the operation of the hydraulic turbine and actuators for the second hydraulic unit;

2. Adding equations that describe the electrical components of both hydraulic units to establish a GPFR connection.

The resulting mathematical model reflects the interaction of two synchronous machines (Fig. 4).

In addition to the equations for the second generator, the mathematical model of the single-machine system in terms of stator winding reaction equations, asynchronous torques for each generator, and the regulating effect of the remote load has been finalized.

To visualize the interaction between two generators and the changes in their frequency, the mathematical model incorporates an emergency disturbance of a 100 MW power outage in the power system. Taking into account all the damping components described, the frequencies of the power system and individual generators alter as outlined in Figure 4.4. In the event of a power deficit, non-damped oscillations are absent, and both system and generator frequencies decrease to 49.15 Hz within 10 seconds, without assistance from regulating devices.

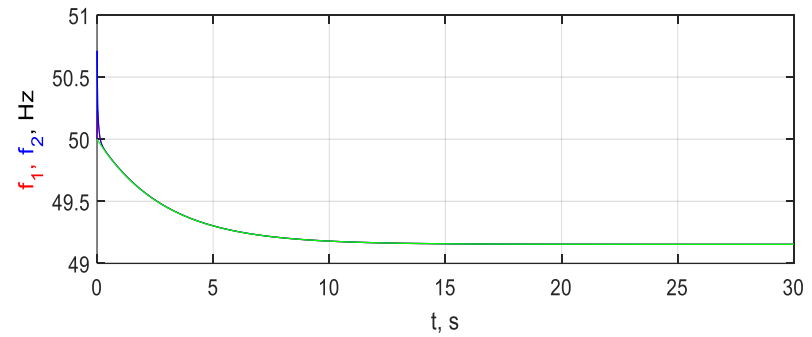


**Fig. 4.** The result of the functioning of a mathematical model containing two synchronous machines.

## 4 Conclusion

This paper discusses the process of general primary frequency control and its performance issues. The study's relevance is supported by multiple works by scientists confirming undamped frequency oscillations in GPFR. In the article, based on the analysis of the works of scientists and regulatory documentation [14], an exhaustive description and confirmation of the research problem associated with the occurrence of undamped frequency oscillations during GPFR is given. The main causes of undamped oscillations are associated with the imprecise tuning of automatic regulators and the deficiencies in control methods.

The main objective of the article was to analyze the transient processes that occur during the GPFR, which is the reason for the description of the development of a mathematical model of the power system. The primary aim of this project is to develop a multifunctional mathematical model for investigating transients at GPFR, equipped with a flexible interface. The model is designed as an analogous simulation of the Norilsk-Taimyr power system, capable of selecting various types of regulation and control laws integrated into regulators' algorithms. The entire process of regulating frequency during different external impacts will be displayed. The next step in the modelling process is to extend the simulated power system to a complete power system encompassing two hydroelectric power plants, namely Ust-Khantai and Kurey HPPs. Each plant will comprise multiple generators. Additionally, a

frequency regulator equipped with static control will serve as automation for one plant whereas a regulator with astatic control will operate the second one.

The reported study was supported by Russian Science Foundation, research project No. 22-79-00181.

## References

1. A. B. Barzam, *System automation [Sistemnaja avtomatika] (in Russian)*, Moscow: Energoatomizdat Publ., p. 446 (1989).
2. N. I. Ovcharenko, *Power system automation [Avtomatika energosistem] (in Russian)*, University textbook, Moscow: MEI Publ., p. 52 (2016).
3. V. A. Fyodorova, V. F. Kirichenko, G. V. Glazyrin, A. Y. Arestova, *Improving Generators Synchronization Methods Based on the Multifunctional System Implementation*, International Multi-Conference on Engineering, Computer and Information Sciences (SIBIRCON–2022), pp. 2100–2105 (2022).
4. Fyodorova V. et al. *Application of Automatic Device for Generator Connection to the Network by Method of Accelerated Synchronization*, IEEE 23 International Conference of Young Professionals in Electron Devices and Materials (EDM), pp. 461–466 (2022).
5. Kas'yanov S. E., Gurikov O. V., *Features of primary frequency control in power system with active power feedback [Osobennosti pervichnogo regulirovaniya chastoty v energosisteme s obratnoj svyaz'yu po aktivnoj moshchnosti] (in Russian)*, International Conference “Electric power industry through the eyes of youth”, pp. 282–285 (2018).
6. Plotnikov L. et al. *An Indirect Method for Determining the Local Heat Transfer Coefficient of Gas Flows in Pipelines*, Sensors, **22**, 6395 p (2022).
7. Gurikov O. V., Smirnov A. N., Andrianov D. I., *Improving the algorithms of the automatic control system for the turbines of the Kola NPP to ensure stable operation of the power system [Sovershenstvovanie algoritmov sistemy avtomaticheskogo regulirovaniya turbin Kol'skoj AES dlya obespecheniya ustojchivoj raboty energosistemy] (in Russian)*, Proceedings of the Scientific and Technical Center of the Unified Energy Systems, **2**, pp. 25–36 (2018).
8. Y. Xu, W. Bai, *Research on Suppression of Ultra-Low Frequency Oscillation of High Hydropower Proportion System by DC Frequency Limiter Controller*, 2019 IEEE 8th International Conference on Advanced Power System Automation and Protection (APAP), pp. 1780–1783 (2019).
9. Y. Shen et al., *Characteristic Analysis of Primary Frequency Modulation in Power System Under Different Types of Active Disturbance*, 2018 2nd IEEE Conference on Energy Internet and Energy System Integration (EI2), pp. 1–5 (2018).
10. J. Gao et al. *Frequency Stability Analysis and Control of AC/DC System*, 2019 16th International Computer Conference on Wavelet Active Media Technology and Information, pp. 392-399 (2019).
11. L.I.U. Qin et al., *Emergency control strategy of ultra-low frequency oscillations based on WAMS*, 2019 IEEE Innovative Smart Grid Technologies-Asia (ISGT Asia), pp. 296–301 (2019).
12. W. Li et al. *UHVDC Islanded Operation System Ultralow-Frequency Oscillation and Its Countermeasures*, IEEE Canadian Journal of Electrical and Computer Engineering, pp. 110–117 (2021).

13. D. Rimorov et al. *Inter-area oscillation damping and primary frequency control of the New York state power grid with multi-functional multi-band power system stabilizers*, 2016 IEEE Power and Energy Society General Meeting (PESGM), pp. 1–5 (2016).
14. A. Delavari, I. Kamwa, *Sparse and resilient hierarchical direct load control for primary frequency response improvement and inter-area oscillations damping*, IEEE Transactions on Power Systems, **5**, pp. 5309–5318 (2018).
15. State Standard 55890-2013. *United power system and isolated power systems. Operative-dispatch management. Frequency control and control of active power. Norms and requirements [Edinaya energeticheskaya sistema i izolirovanno rabotayushchie energosistemy. Operativno-dispetcherskoe upravlenie regulirovanie chastoty i peretokov aktivnoj moshchnosti. Normy i trebovaniya] (in Russian)*, Russian power system operator Publ., 51 p. (2014).
16. N.T. Trinh, M. Zeller, and I. Erlich, *Coordination of Functional Controllers in a Multiterminal MMC-VSC-HVDC System Control*, 2018 IEEE PES Innovative Smart Grid Technologies Conference Europe (ISGT-Europe), pp. 1–5 (2018).